

A General Channel Model for Visible Light Communications in Underground Mines

Jia Wang¹, Ahmed Al-Kinani², Wensheng Zhang¹, Cheng-Xiang Wang³, Li Zhou^{1,*}

¹Shandong Provincial Key Lab of Wireless Communication Technologies, Shandong University, Qingdao, Shandong 266237, China

²Technical Affairs Department, Iraqi Ministry of Communications, Baghdad 10013, Iraq

³State Key Laboratory of Mobile Communications, Southeast University, Nanjing 210096, China

* The corresponding author, email: zhou_li@sdu.edu.cn

Abstract: In underground mines, visible light communication (VLC) system is a promising method to realize effective communication, which supports communication and illumination at the same time. Therefore, adequate research of underlying physical propagation phenomenon should be carried out to realize VLC system in underground mines. To design VLC system and evaluate its performance, accurate and efficient channel models, including large-scale fading and scattering characteristics, are needed to be established. However, the characteristics of the underlying VLC channels about fading and scattering have not been sufficiently investigated yet. In this paper, a path loss channel model, based on the recursive model, is proposed precisely. Its path loss exponent is determined by three different trajectories, which is studied in the mining roadway and working face environment. Besides, the shadowing effect for VLC has been modelled by a Bimodal Gaussian distribution in underground mines. Considering the number of transmitters in line-of-sight (LoS) as well as non-line-of-sight (NLoS) scenarios, our simulation illustrates the fact that, as the curve fitting technique is employed, the path loss displays a linear behavior in log-domain.

The path loss expression is derived, it is related to the distance. Finally, root mean square (RMS) delay spread and Mie scattering in underground mines are analyzed.

Keywords: underground mines; visible light communications; channel modeling; path loss; shadowing; delay spread.

I. INTRODUCTION

The underground mining industry promotes the development of the global economy significantly, but there are some restrictions for its progress due to the presence of toxic gases, substances, and dust, which are generated from mining and production. Therefore, reliable communications, monitoring, and tracking systems are urgently needed to guarantee safety and maximize productivity in underground mines. In other words, maintaining information is one of the biggest challenges during mining operations. The information includes detecting hazardous gases and/or smoke, monitoring mining machinery are included, of which the most pivotal is how to monitoring miners and locating them as disaster occurs. The most common communication systems in underground mines include personal hand-

Received: Dec. 22, 2017

Revised: Mar. 23, 2018

Editor: Xiaotian Zhou

In this paper, the path loss and shadowing of VLC channels in underground mines have been studied.

phone system (PHS), CDMA mobile communication system, and through-the-earth (TTE). In underground mines, hard-wires, wireless or a combination of both are applied to realize information exchange. Since the structure of underground mines is complex, the traditional wire communication systems, including twisted pair, coaxial, and fibre-optic, are very susceptible to be damaged. Besides, a sharp attenuation of radio wave transmission makes the existing wireless communication systems not to be directly employed [2]. And another challenge for miner to see potential surrounding hazards is the poor lighting condition. All these factors make the study on visible light communication (VLC) to be a promising research hotspot. Anyhow, infrared, bluetooth, ultra-wideband (UWB) and ZigBee have been applied in underground mining communications (UMCs) to some degree [3], [4].

However, VLC is superior to the later technologies for short range communications in some aspects, i.e., 1-10 m [5], [6]. VLC technology has many advantages, such as unlicensed spectrum, low-cost, and supporting high data rate [7], [8], which are summarized as follows: First, as it is well known that the air contains a lot of dust, water vapour and flammable gas in underground mines, these factors seriously interfere with the transmission of electromagnetic waves, and limit the use of wireless communication equipment. However, VLC technology has an important characteristic of electromagnetic interference resistance. Then, LED lamps are cold light sources and have long life, which are convenient for workers to greatly reduce the risk of accidents caused by downhole lighting maintenance risks. VLC is expected to be an important part of the next generation wireless communications in underground mines. VLC in underground mines are based on the off-the-shelf light-emitting diodes (LEDs), which can be equipped on the ceiling of the underground mining or mounted on miner's helmet to establish a VLC link between either the miners and infrastructures or with other miners, respectively. The transparent boxes fixed on

the communication interfaces will prevent the dust and dirty in underground mines. There is a growing literature related to indoor VLC channels characterization including path loss and shadowing. But only a few authors have focused on VLC channels characterization for UMCs such as [5], [9]. However, VLC channel path loss and shadowing effect have not been considered in previous studies. In this study, we extend the work in [10] to characterize the optical channel path loss and shadowing in underground mines considering the working face and mining roadway environments. To the best of the authors' knowledge, there is no previous work addressing path loss and shadowing of VLC channels in underground mines.

Compared with indoor communication environment, the communication environment in underground mines is more complicated. Due to the presence of minute particles in the air which contain a large amount of water vapor, flammable gas and particulate matter, the scattering seriously affect the optical signal transmission [9]. As flammable gas and water vapor mainly absorb light with a wavelength of about $750 \mu\text{m}$ and the spectrum of visible light is 385-789 THz [11], both the absorption and the scattering of flammable gas and water vapor are negligible in the underground mines. On the other hand, the size of particulate matter suspended in the atmosphere is approximately equal to the wavelength of visible light. Thus, the particulate matter generate Mie scattering which is the main factor causing attenuation of light intensity. In this paper, we follow the Mie scattering theory to quantitatively analyze the optical signal decays and the influence of attenuation after the scattering of particulate matter in the underground mines.

The rest of the paper is organized as follows. Section II introduces VLC system model and path loss in underground mines. Section III derives the impact of Mie scattering on the VLC channel. Results and discussions are presented in Section IV. Conclusions are finally drawn in Section V.

II. A VLC PATH LOSS MODEL IN UNDERGROUND MINES

Usually, the underground mines can be divided into mining roadway and working face. In order to represent these environments easily, horseshoe shape and rectangle chamber with 2 m width are considered to model mining roadway and working face, respectively. In the proposed system model, the underground mines are equipped with LED lamps for the purpose of illumination and communication simultaneously, as presented in figure 1. The key parameters of the proposed underground mines VLC system are detailed in table 1.

In order to optimize the communication effect in underground mines, the light intensity in the space should be distributed as uniformly as possible. Multiple LED lamps should be installed on the ceiling of underground mines. Compared with the distance between LED arrays, the size of LED lamps can be ignored. Thus, the LED array can be considered as an entirety and the luminous power of each LED array is equal to the sum of the LED lamps' luminous powers. In this article, each LED array N is composed of 10×10 identical LED lamps. To simplify the calculation, LED lamps in the same LED array transmit the same signal. So, the number of transmitters can be regarded as the number of LED arrays. Besides, the positions of transmitters (TP) are marked in table 1.

2.1 VLC system model

Assuming that each LED lamp has the same Lambertian radiation pattern [12], the angular distribution $S(\phi)$ of the radiation intensity pattern is given as [13]

$$S(\phi) = \begin{cases} \frac{(m+1)}{2\pi} \cos^m(\phi) & \text{if } \phi \in \left[\frac{-\pi}{2}, \frac{\pi}{2} \right] \\ 0 & \text{otherwise.} \end{cases} \quad (1)$$

Here, ϕ is the incident angle and m is the Lambertian mode number which is related to the LED semi-angle ϕ_1 , m is given as

$$m = \frac{-\ln 2}{\ln \left(\cos \phi_1 \right)}. \quad (2)$$

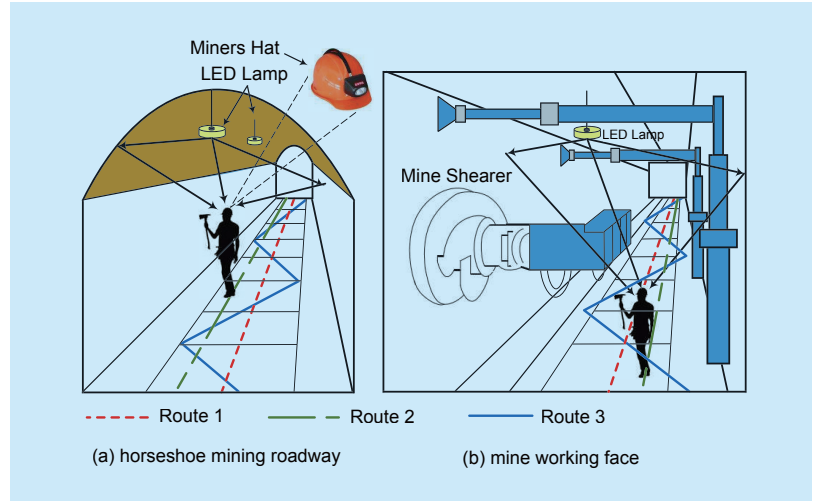


Fig. 1. System model.

Table I. The key parameters.

System Model Parameters	
Mining Roadway}}	
Dimensions	2 m × 5 m × 3.7 m
Radius	1 m
Coordinates of the transmitter	(0,0,1)
The location of Route 1	$x=0, z=-1$
The location of Route 2	$x=0.5, z=-1$
The location of Route 3	$-0.6 \leq x \leq 0.6, z=-1$
Working Face	
Dimensions	2 m × 5 m × 4.7 m
Coordinates of the single transmitter	(0,0,-2)
Coordinates of the four transmitters with TP1	(-0.5,-1.25,1)
Coordinates of the four transmitters with TP2	(0.5,1.25,1)
Coordinates of the four transmitters with TP3	(0.5,-1.25,1)
Coordinates of the four transmitters with TP4	(-0.5,1.25,1)
The location of Route 1	$x=0, z=-2$
The location of Route 2	$x=0.5, z=-2$
The location of Route 3	$-0.6 \leq x \leq 0.6, z=-2$
Other Parameters	
Height of receiving plane	1.7 m
Number of LED lamps ($N=1$)	100
Semi-angle at half power	70°
Concentrator refractive index (n)	1.5
Reflection coefficient (ρ)	0.8
Photodiode area (A_r)	1 cm ²
Field of view (FoV)	60°
Band-pass filter of transmission (T_s)	1

The channel impulse response of the line-of-sight (LoS) component in the underground mines can be given as [13]

$$h_{\text{LoS}}(t) = \frac{A_r(m+1)}{2\pi d_0^2} \cos^m(\phi_0) T_s(\theta_0) g(\theta_0) \times \cos(\theta_0) \delta\left(t - \frac{d_0}{c}\right). \quad (3)$$

Here, A_r is the optical detector area, the distance between the transmitter and the receiver is d_0 , and the speed of the light in free space is c . In addition, the transmit angle is ϕ_0 and the receive an θ_0 , where $\phi_0 < 90^\circ$, $\theta_0 < FOV$, and $d_0 \gg \sqrt{A_r}$, respectively. The Dirac function is $\delta\left(t - \frac{d_0}{c}\right)$. To compute the length of propagation path between the reflections, let the angles of incidence and received be ϕ_1, ϕ_i and θ_1, θ_j , and d_ε is the distance generated by source element and destination, then the impulse response of the receiver with N transmitters and the k -th order reflections can be expressed as

$$h_{\text{NLoS}}^k(t) = \sum_{i=1}^N \int \frac{100 \cos^m(\phi_1) \prod_2^{k+1} \cos(\phi_i) \prod_1^{k+1} \cos(\theta_j)}{2\pi^{k+1} \prod_1^{k+1} d_\varepsilon^2} \times A_{\text{ref}}^k A_r(m+1) \rho^k T_s(\theta_{k+1}) g(\theta_{k+1}) \times \text{rect}\left(\frac{\theta_{k+1}}{FOV}\right) \delta\left(t - \frac{d_i + d_j}{c}\right) dA_{\text{ref}},$$

where ρ is the reflectance coefficient and $\text{rect}\left(\frac{\theta_{k+1}}{FOV}\right)$ is a decision function.

2.2 Path loss model

To mitigate the effect of fading, the large scale fading and small scale fading are commonly considered carefully in wireless communication. Unlike in radio frequency (RF) wireless communication, the effect of multipath fading is not considered in VLC, because the surface area of VLC detectors are typically millions of square wavelengths of visible light [5]. In the underground mines VLC system, the path loss can be calculated as [14]

$$PL = -10 \log_{10} \left(\int_0^\infty h(t) dt \right). \quad (5)$$

In a typical free space system, the logarithm distance path loss is a generic model in both RF communication and optical wireless communication. When the distance d between transmitter and receiver is larger than the reference distance d_r , the path loss can be expressed as [15]

$$PL = PL(d_r) + 10n \log_{10} \left(\frac{d}{d_r} \right) + \chi. \quad (6)$$

Here, n is the the path loss exponent and χ is a random variable that accounts for shadowing effects.

2.3 The effect of shadowing

In this scenario, the LED lamps that are fixed on the mine ceiling are regarded as transmitters to provide communication and the receivers are mounted on the ground. The situation that a miner would block transmission of light between LED lamp and other receivers is unavoidable, so the effect of shadowing of a person must be researched. To simplify the model, a person can be identified as a cylinder or a cuboid whose height (about 1.70 m) is larger than its lateral size (about 0.35 m). In view of this, the light diffraction is taken into account to be the Bimodal Gaussian Effect (BGE) which is resulted from the two vertical edges. The BGE affects the impulse response in underground mine, if $h_{1\text{LoS}}(t)$ and $h_{2\text{LoS}}(t)$ are regarded as the impulse response of the two edges, then received energy is [16] [17]

$$E_{\text{receive}} = \int_0^T \{s(t) \times [h_{1\text{LoS}}(t) + h_{2\text{LoS}}(t)]\}^2 dt. \quad (7)$$

Here, $s(t)$ is signal from the LED lamp and T is the time duration about signal transmission.

2.4 Root mean square(RMS) delay spread

Inter-symbol interference (ISI) induced by multipath dispersion has a significant impact on channel capacity. The RMS delay spread is a parameter which can quantify the degree of the time-dispersive properties of multipath dispersion. The mean excess delay μ_τ can be calculated from the channel impulse response as

$$\mu_\tau = \frac{\sum_i \tau_i h_i^2(t)}{\sum_i h_i^2(t)}. \quad (8)$$

Here, τ_i is the duration of time. Then the channel RMS delay spread is given by σ_τ [13]

$$\sigma_\tau = \sqrt{\frac{\sum_i (\tau_i - \mu_\tau)^2 h_i^2(t)}{\sum_i h_i^2(t)}}. \quad (9)$$

III. MIE SCATTERING IN UNDERGROUND MINES

The idea of Mie scattering in underground mines is meaningful for VLCs. According to the standards set by the government [5], the particulate matter concentration in underground mines generally does not exceed 10 mg/m³, of which the amount of particulate matter produced by the working face is the largest. The particulate matter generates the absorption and scattering when the visible light goes through the particulate matter. It is worth to mention that we assume that the particulate matter is spherical and evenly distributed in the air, the Mie scattering theory can be useful to study the particulate matter scattering characteristics in underground mining.

When visible light is emitted from the LED lamp, it will propagate a distance d before it is scattered. We assume LED lamp obeys the Lambert radiation distribution and the Lambertian modes m of all LED lamps are the same. The illuminance $I(\phi)$ is given as [10]

$$I(\phi) = \sum_{i=1}^N i I_o \cos^m(\phi). \quad (10)$$

Here, the number of LED is N and the centre luminous intensity of the LED is I_o . The luminous intensity $E(\phi)$ in angle ϕ is given as [18]

$$E(\phi) = \frac{I(\phi)}{d^2}. \quad (11)$$

According to the theory of Mie scattering, when the light is shining on spherical particle, the intensity of scattering light received at the observation point can be divided into the ver-

tical and the parallel components. Therefore, the intensity of scattering light I_{sca} can be expressed as [18]

$$I_{sca} = I_\perp + I_\parallel. \quad (12)$$

In equation (12), I_\perp and I_\parallel represent the vertical component and the parallel component, respectively. In Mie Scattering theory, if the distance between the spherical particle and the observe point is set as r , the polarization angle of the incident light is set as θ and the corresponding scattering angle is set as φ , then the intensity of scattering light can be expressed as [18] [19]

$$I_\perp = \frac{I(\phi)\lambda^2}{4\pi^2 r^2} f_1 \sin^2 \theta \quad (13)$$

$$I_\parallel = \frac{I(\phi)\lambda^2}{4\pi^2 r^2} f_2 \cos^2 \theta, \quad (14)$$

where f_1 and f_2 are intensity functions respectively, they are related to the scattering angel, size of the spherical particle, as well as refractive index of the spherical particle, so they can be expressed as [13]

$$f_1 = |g_1(n, \varphi, \beta)|^2 \quad (15)$$

$$f_2 = |g_2(n, \varphi, \beta)|^2. \quad (16)$$

Here, β is the diametric parameter of the particle, i.e.,

$$\beta = \frac{\pi d}{\lambda}, \quad (17)$$

and q standards for the plural refractive index of particles. The g_1 and g_2 are amplitude functions, which can be shown as [13]

$$g_1 = \sum_{m=1}^{\infty} \frac{2m+1}{m(m+1)} [a_m \gamma_m + b_m \chi_m] \quad (18)$$

$$g_2 = \sum_{m=1}^{\infty} \frac{2m+1}{m(m+1)} [a_m \chi_m + b_m \gamma_m], \quad (19)$$

where a_m and b_m are scattering coefficients of Mie Scattering, γ_m and χ_m are scattering angle functions. These parameters are critical for Mie Scattering calculates. The expressions of a_m and b_m are [13]

$$a_m = \frac{\Psi_m(\beta)\Psi'_m(q\beta) - I\Psi'_m(q\beta)\Psi_m(q\beta)}{\xi_m(\beta)\Psi'_m(q\beta) - I\xi'_m(q\beta)\Psi_m(q\beta)} \quad (20)$$

$$b_m = \frac{m\Psi_m(\beta)\Psi'_m(q\beta) - \Psi'_m(q\beta)\Psi_m(q\beta)}{m\xi_m(\beta)\Psi'_m(q\beta) - \xi'_m(q\beta)\Psi_m(q\beta)}, \quad (21)$$

with

$$\Psi_m(z) = \left(\frac{z\pi}{2}\right)^{\frac{1}{2}} J_{m+\frac{1}{2}}(z) \quad (22)$$

$$\xi_m(z) = \left(\frac{z\pi}{2}\right)^{\frac{1}{2}} H_{m+\frac{1}{2}}(z). \quad (23)$$

Here, z stands for β or $n\beta$, $J_{m+\frac{1}{2}}(z)$ and $H_{m+\frac{1}{2}}$ represent Bessel function and the second kind of Hankel function, respectively.

The scattering angle functions are only related to scattering angle and can be expressed as [13]

$$\gamma_m = \frac{dP_m(\cos\varphi)}{d\cos\varphi} \quad (24)$$

$$\chi_m = \frac{d}{d\varphi} P_m^{(1)}(\cos\varphi), \quad (25)$$

where, $P_m^{(1)}(\cos\varphi)$ is the first order of the first kind Legendre function.

The scattering coefficient Q_s and extinction coefficient Q_e can be deduced from the above expressions as

$$Q_{sca} = \frac{2}{\beta^2} \sum_{m=1}^{\infty} (2m+1) (|a_m|^2 + |b_m|^2) \quad (26)$$

$$Q_{ext} = \frac{2}{\beta^2} \sum_{m=1}^{\infty} (2m+1) R_e(a_m + b_m). \quad (27)$$

IV. RESULTS AND DISCUSSIONS

To evaluate the performance of different communication scenarios in underground mines, the channel characteristics for both environments are analyzed. The results are presented in table II by applying the curve fitting techniques for 3 routes in mining roadway and 3 routes of working face.

4.1 Path loss

The path loss of VLC channel is computed in both mining roadway and working face. We choose three movement trajectories in underground mines to calculate the LoS path loss and NLoS path loss, as presented in figure 1. Moreover, the path loss exponent n has been obtained from (6) by applying the curve fitting technique on the simulation values of path loss results which are obtained from (5).

1) *LoS Path Loss*: The simulation results of LoS path loss under three movement trajectories in mining roadway and working face are presented in figure 2 and figure 3 respectively. As expected, the path loss exhibits a linear behavior in log-domain via the curve fitting techniques which are applied in the figure 2 and figure 3. In addition, the values of the norm of residuals are small on Route 1, Route 2, and Route 3 which are 10.24×10^{-5} , 10.65×10^{-5} , and 31.24×10^{-5} in mining roadway. Meanwhile, the values of norm of residuals in working face which approximately equal 8.50×10^{-5} , 7.77×10^{-5} , and 23.58×10^{-5} are smaller than that in mining roadway, respec-

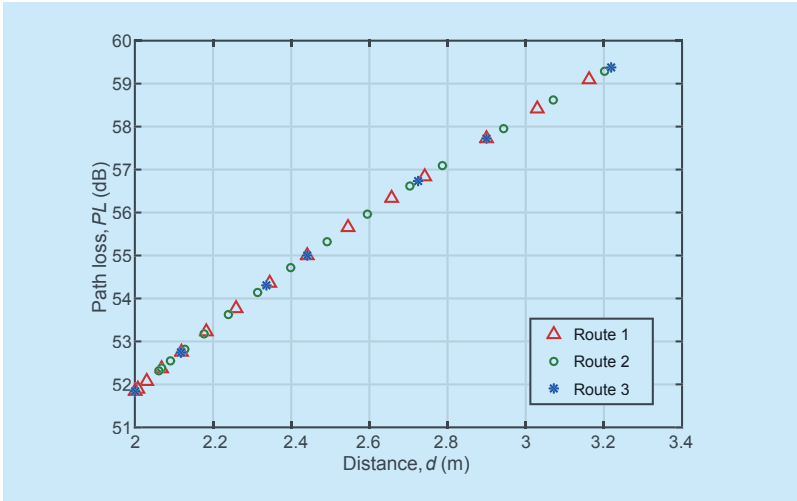


Fig. 2. LoS path loss estimation in mining roadway.

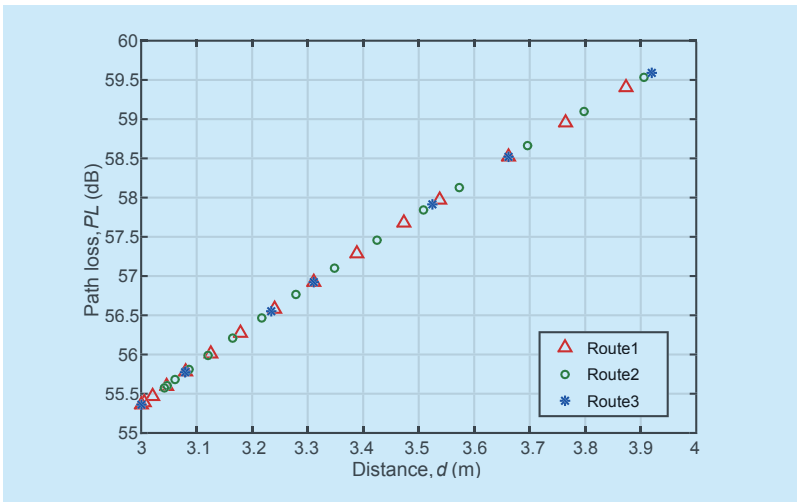


Fig. 3. LoS path loss estimation in working face.

tively. Moreover, it can be noticed in table 2 that the path loss exponents have the same value, which is equal to 3.64 on Route 1, Route 2, and Route 3 with the different reference distance. Hence, the shape of communication scenarios and the different reference distance have no influence on the value of path loss exponent. One obvious phenomenon that some discrete points of Route 1 and Route 3 are coincident in figure 2 and figure 3. This can be explained that the Route 3 of the polylines is partly going through the Route 1 which is in the middle of mine. Since Route 1 exhibits a higher linear behavior, it is used to develop the model for LoS path loss in mining roadway and working face. Thus, the LoS path loss equations as a function of distance d between the transmitter and receiver in mining roadway and working face can be written as follows:

$$PL_{\text{Mining Roadway}}^{\text{LoS}} = 51.84 + 36.46 \log_{10} \left(\frac{d_1}{2} \right) + \chi, \quad (28)$$

and

$$PL_{\text{Working Face}}^{\text{LoS}} = 55.36 + 36.46 \log_{10} \left(\frac{d_2}{3} \right) + \chi. \quad (29)$$

Here, $d_1 \geq 2m$ and $d_2 \geq 3m$.

4.2 NLoS path loss estimation

The simulation results in figure 4 and figure 5 are related to NLoS path loss with three movement trajectories in underground mines which are correspondingly estimated for distances from 2 m to 3.22 m and 3 m to 3.92 m away from the respective operational transmitter in mining roadway and working face, respectively. To simplify the calculation, only first reflection is considered. It can be seen that the LoS path loss estimation is better than NLoS path loss estimation obviously on the linear behavior in log-domain in figure 2 and figure 4. However, because of the increasing reflection walls, the path loss exponent of mining roadway is larger than that of working face. Therefore, the NLoS path loss equation along Route 1 in mining roadway and working face are determined as follows:

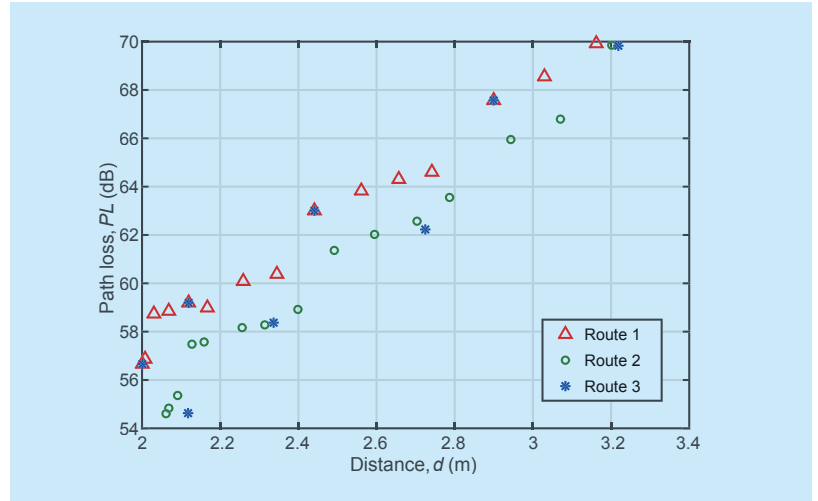


Fig. 4. NLoS path loss estimation in mining roadway.

Table II. Estimated parameters for the path Loss model.

LoS path loss estimation in mining roadway		
Route	Fitting equation	Norm of residuals
1	$= 51.84 + 36.46 \log_{10} \left(\frac{d}{2} \right)$	1.025×10^{-4}
2	$= 52.32 + 36.46 \log_{10} \left(\frac{d}{2} \right)$	1.065×10^{-4}
3	$= 51.84 + 36.46 \log_{10} \left(\frac{d}{2} \right)$	3.124×10^{-4}
NLoS path loss estimation in mining roadway		
Route	Fitting equation	Norm of residuals
1	$= 57.18 + 61.55 \log_{10} \left(\frac{d}{2} \right)$	2.442
2	$= 55.17 + 69.72 \log_{10} \left(\frac{d}{2} \right)$	2.799
3	$= 55.50 + 67.20 \log_{10} \left(\frac{d}{2} \right)$	4.935
LoS path loss estimation in working face		
Route	Fitting equation	Norm of residuals
1	$= 55.36 + 36.46 \log_{10} \left(\frac{d}{3} \right)$	0.8497×10^{-4}
2	$= 55.68 + 36.46 \log_{10} \left(\frac{d}{3} \right)$	0.7768×10^{-4}
3	$= 55.36 + 36.46 \log_{10} \left(\frac{d}{3} \right)$	2.358×10^{-4}
NLoS path loss estimation in working face		
Route	Fitting equation	Norm of residuals
1	$= 53.44 + 54.47 \log_{10} \left(\frac{d}{3} \right)$	0.7795
2	$= 54.13 + 56.13 \log_{10} \left(\frac{d}{3} \right)$	0.6885
3	$= 53.56 + 58.43 \log_{10} \left(\frac{d}{3} \right)$	0.9971

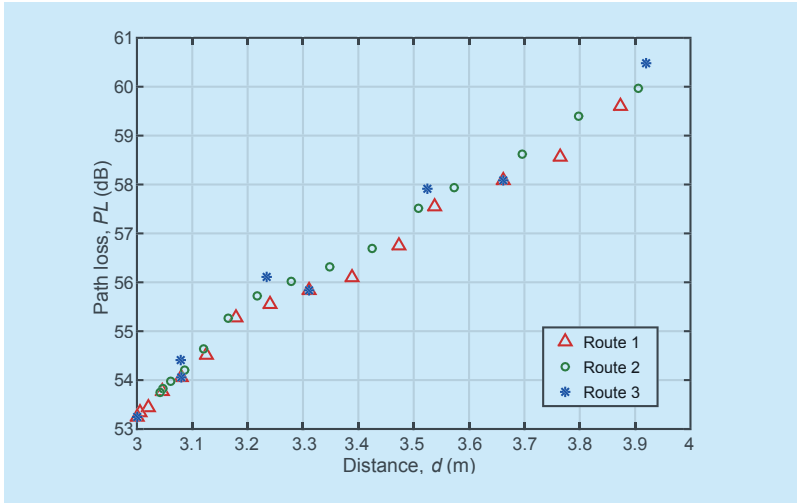


Fig. 5. NLoS path loss estimation in working face.

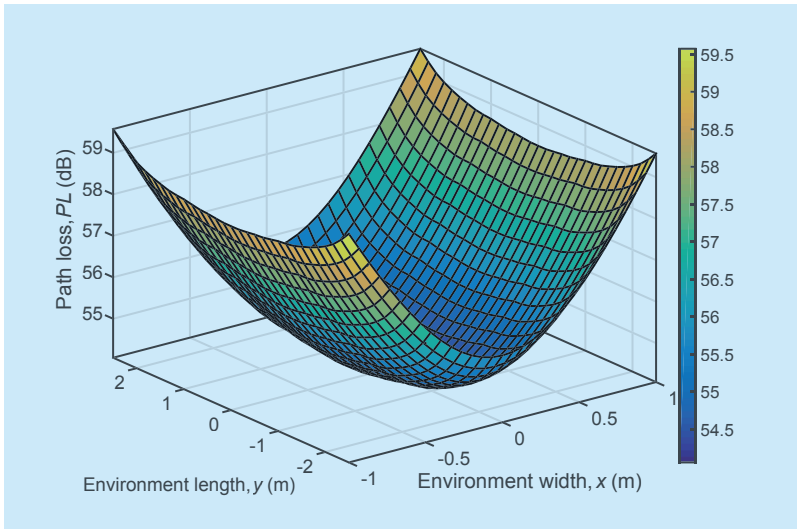


Fig. 6. Path loss distribution for a single transmitter in working face.

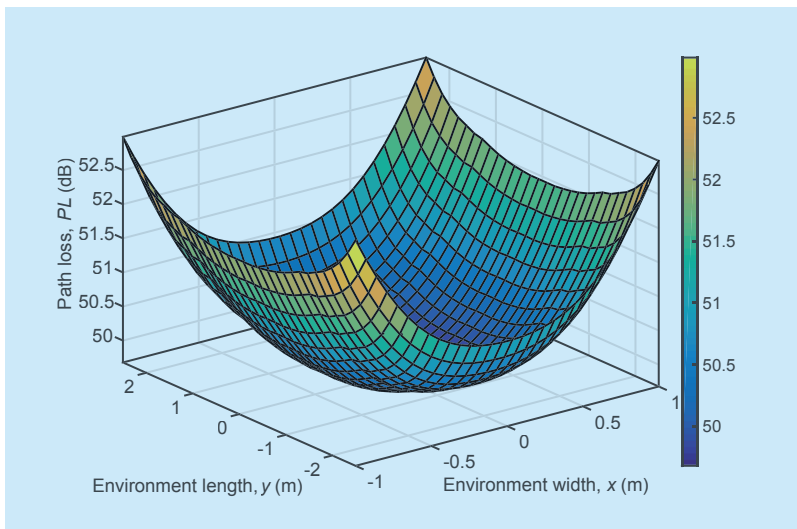


Fig. 7. Path loss distribution for four transmitters in working face.

$$PL_{\text{Mining Roadway}}^{\text{NLoS}} = 57.18 + 61.55 \log_{10} \left(\frac{d_1}{2} \right) + \chi, \quad (30)$$

and

$$PL_{\text{Working Face}}^{\text{NLoS}} = 53.44 + 54.47 \log_{10} \left(\frac{d_2}{3} \right) + \chi. \quad (31)$$

Here, $d_1 \geq 2m$ and $d_2 \geq 3m$.

As observed from figure 6 and figure 7, the path loss varies with the number of transmitters and user location. Here, the maximum values and minimum values of path loss in received plane are 59.57 dB and 54.06 dB with a single transmitter in working face, which are 6.58 dB and 4.38 dB larger than that with four transmitters, respectively. As shown in figure 6, the path loss increases obviously as receiver away from transmitter. This is due the fact that transmitter have been equipped at the center of environment. Thus, the middle of received plane has the minimum path loss compared with the other positions in figure 6 and figure 7.

4.3 The effect of shadowing

A person's shadowing influences the communication between the transmitters and the receivers, so the BGE model in figure 10 is introduced to the VLC in underground mine. The expression (7) of received energy is given, which explains how the shadowing affects the VLC in underground mine. The probability of error caused by shadowing will be affected by varying the received signal energies as well as its variances for the BGE. As depicted in figure 10, the values μ_0 and μ_1 are means of the first and second combined Gaussian distributions, respectively. Due to symmetry of the cylinder, one can conclude that the standard deviations δ are the same equalling. The average probability of error is given by [18]

$$P_{re} = R \left(\frac{\mu_1 - \mu_0}{2\delta} \right). \quad (32)$$

Here, in order to simplify the calculation, the function R_x is introduced which is given as [18]

$$R_x = \int_{\frac{\mu_0 + \mu_1}{2}}^{\infty} \frac{1}{\sqrt{2\pi}\delta} \exp \left[-\frac{(x - \mu_0)^2}{2\delta^2} \right] dx. \quad (33)$$

The probability of error will decrease when the received signal power increases, as a result of increasing the LED transmitted power.

4.4 RMS delay spread

RMS delay spread for the cases of a single transmitter and four transmitters are illustrated in figure 8 and figure 9, respectively. It can be noticed that the maximum values are 0.4500 ns and 1.6546 ns for a single transmitter and four transmitters, respectively. Likewise [20], the minimum values are 0.1781 ns and 0.2381 ns, respectively. As shown in figure 8 and figure 9, the RMS delay spread distribution [21] is not uniform because the model of the working face is not closed cuboid. Reflections from the right wall and left wall are not counted. However, taken LoS and NLoS components into consideration, the RMS delay spread decreases as receiver goes away from transmitter as illustrated in figure 8 and figure 9.

V. CONCLUSIONS

In this paper, the path loss and shadowing of VLC channels in underground mines have been studied. The recursive channel model VLC has been introduced in both mining roadway and working face with different numbers of transmitters. According to Mie scattering theory, the particulate matter will influence the illumination intensity and affect the performance of VLC systems in mines. To be specific, the path loss exponents over three different trajectories in LoS and NLoS scenarios have been calculated. And it has been gotten from simulation that path loss is linear in log-domain. Besides, no matter in mining roadway or working face, the value of path loss exponent of NLoS is larger than that of LoS. From our studies, multi-modal Gaussian distribution of the received power has appeared when more severe and complicated shadowing emerges. Besides, as receiver moves away from the transmitter, the RMS delay spread will decrease.

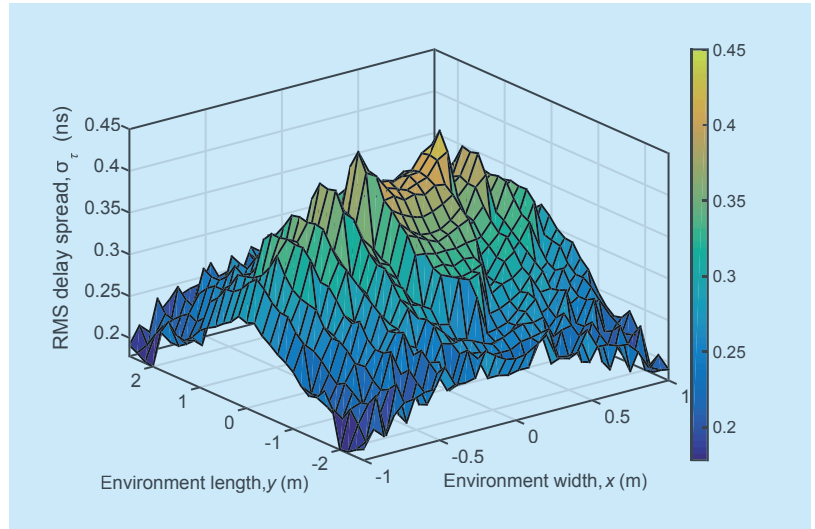


Fig. 8. RMS delay spread distribution for a single transmitter in working face.

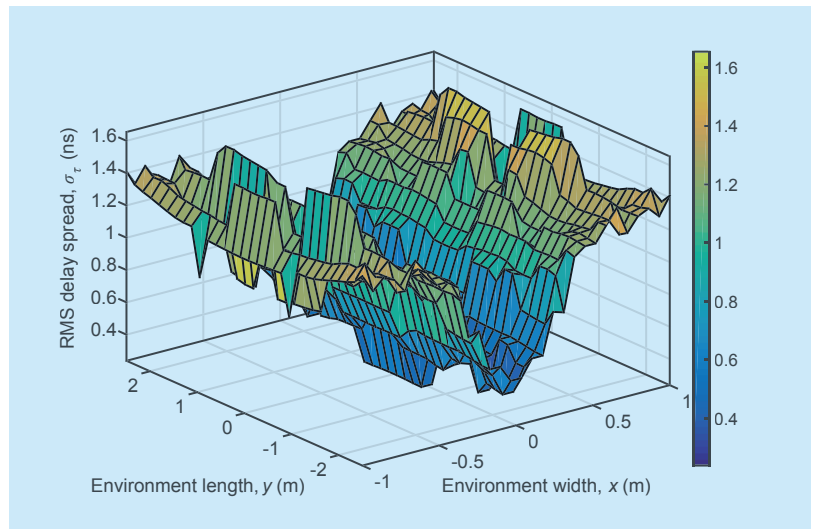


Fig. 9. RMS delay spread distribution for four transmitters in working face.

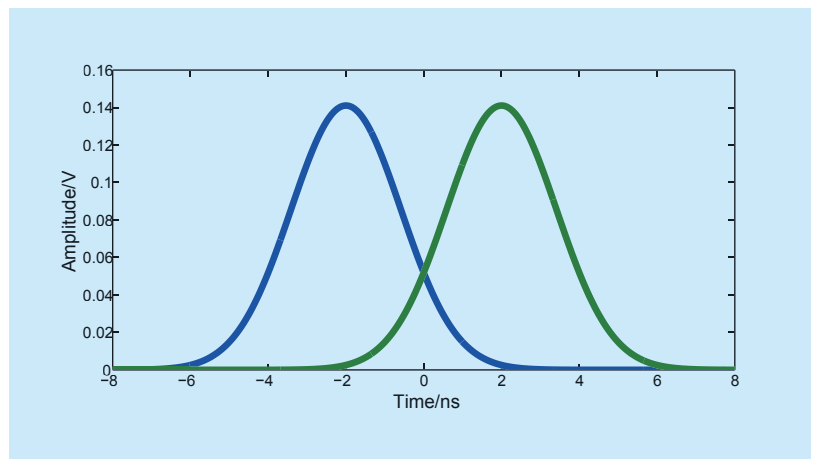


Fig. 10. Bimodal gaussian function.

ACKNOWLEDGEMENTS

The authors would like to acknowledge the support from the National Natural Science Foundation of China (Grant No. 61371110), Key R&D Program of Shandong Province (Grant No. 2016GGX101014), EU H2020 RISE TESTBED project (Grant No. 734325), and the Fundamental Research Funds of Shandong University (No. 2017JC029).

References

- [1] Yarkan S, Guzelgoz S, and Arslan H, *et al.* Underground mine communications: A survey[J]. *IEEE Commun. Surveys Tuts.*, 2009, 11(3): 125-142.
- [2] Ren P and Qian J. A power-efficient clustering protocol for coal mine face monitoring with wireless sensor networks under channel fading conditions[J], *Sensors*, 2016, 16(6): 1-21.
- [3] Zhang Y, Zhang Y, and Li C. Research of short distance wireless communication technology in the mine underground[C], *Proc. IMCCC'14*: Sept. 2014, Harbin, China. 2014: 955-959.
- [4] Lee K, Park H, and Barry J R. Indoor channel characteristics for visible light communications[J], *IEEE Commun. Lett.*, 2011, 15(2): 217-219.
- [5] Wu G and Zhang J, Demonstration of a visible light communication system for underground mining applications[C], *Proc. IECT'16*: June 2016, Shanghai, China. 2016:1-7.
- [6] Al-Kinani A, Wang C X and Haas H, *et al.* A geometry-based multiple bounce model for visible light communication channels[C], *Proc. IEEE IWCMC'16*: Sept. 2016, Paphos, Cyprus. 2016:31-37.
- [7] Al-Kinani A, Wang, C X and Haas H, *et al.* Characterization and modeling of visible light communication channels[C], *Proc. IEEE VTC'16-Spring*: May. 2016, Nanjing, China. 2016:1-5.
- [8] Miramirkhani F and Uysal M. Channel modeling and characterization for visible light communications[J], *IEEE Photonics Journal*, 2015, 7(6): 1-16.
- [9] Zhai Y and Zhang S. Visible light communication channel models and simulation of coal workplace energy coupling[J], *IEEE Journal of Mathematical Problems in Engineering*, 2015, 27152:1-10.
- [10] Wang J, Al-Kinani A, Zhang W S, and Wang C X, A new VLC channel model for underground mining environments[C], *Proc. IEEE IWCMC'17*: June. 2017, Valencia, Spain.
- [11] Damen M O, Narmanlioglu O, and Uysal M, Comparative performance evaluation of MIMO visible light communication systems[C], *Proc. IEEE SIU'16*: 2016, Zonguldak, Turkey. 2016: 525-528.
- [12] Moreno I and Sun C C, Modeling the radiation pattern of LEDs[J], *Opt. Express*, 2008, 16(3): 1808--1819.
- [13] Z. Ghassemlooy, W. Popoola, and S. Rajbhandari, 1st Ed., *Optical Wireless Communications: System and Channel Modeling with MATLAB*, New York: CRC press, 2013.
- [14] Miramirkhani F, Narmanlioglu O and M. Uysal, *et al.* A mobile channel model for VLC and application to adaptive system design[J], *IEEE Commun. Lett.*, 2017, 21(5): 1035-1038.
- [15] Dimitrov S, Mesleh R and Haas H, *et al.* Path loss simulation of an infrared optical wireless system for aircrafts[C], *Proc. IEEE Globecom'09*: Dec. 2009, Honolulu, USA. 2009: 1-6.
- [16] Farahneh H, Mekhiel C and Khalifeh A, *et al.* Shadowing effects on visible light communication channels[C], *Proc. IEEE CCECE '16*: May 2016, Vancouver, Canada. 2016:1-5.
- [17] Grubor J, Randel S and Langer K D, *et al.* Broad-band information broadcasting using LED-based interior lighting[J], *Journal of Lightwave Technology*, 2008, 26(24): 3883-3892.
- [18] Wu D, Ghassemlooy Z, Rajbhandari S, and Minh H L, Channel characteristics analysis and experimental demonstration of a diffuse cellular indoor visible light communication system[J], *The Mediterranean Journal of Electronics and Communications*, 2012, 8: 1-7.
- [19] C. D. J. Statham, Underground lighting in coal mine[J], *Proc. IEE -Part A: Power Engineering.*, 1956, 103(10): 396-409.
- [20] S Ma, Yang R, Li H, Dong Z, Gu H, and Li S, Achievable rate with closed-form for SISO channel and broadcast channel in visible light communication networks[J], *IEEE/OSA Journal of Lightwave Technology*, 2017, 7: 2778-2728.
- [21] S Ma, Zhang T, Lu S, Li H, Wu Z, and Li S, Energy efficiency of SISO and MISO in visible light communication systems[J], *IEEE/OSA Journal of Lightwave Technology*, 2018, 9: 1-1.

Biographies



Jia Wang, received the B.Sc. degree in communication engineering from Harbin Institute of Technology, China, in 2015, the M.Sc. degree in electronics and communication engineering from Shandong University, Shandong, China, in 2018. Her research interests include channel modelling, visible light communication, channel model for visible light communication, and power line communication. Email: wangjia082111@163.com



Ahmed Al-Kinani, received the B.Sc. degree (Hons.) in laser physics and the M.Sc. degree in optical communications from the University of Technology, Baghdad, Iraq, in 2001 and 2004, respectively, and the Ph.D. degrees in optical wireless communications from the University of Edinburgh and Heriot-Watt University, Edinburgh, U.K., in 2018. He is currently with the Iraqi Ministry of Communications, Baghdad, as a Senior Programmer. His main research interests include wireless channel characterization and modeling for visible light communications. Email: ahmed.alkinani@yahoo.com



Wensheng Zhang, received the Msc degree in Communication and Information Systems from Shandong University, China, in 2005, and the PhD degree in Communication Engineering from Keio University, Japan, in 2011. He has been a Lecturer in School of Communication, Shandong Normal University, China, from 2005 to 2007. In 2011, he was a visiting researcher at Oulu University, Finland. Since 2012, he has been a Lecturer in the School of Information Science and Engineering, Shandong University, China, where he was promoted to an associate Professor in 2016. His research interests are in the areas of random matrix theory and big data analysis, visible light communication networks, intelligent wireless communication systems, and 5G wireless communications. Email: zhangwsh@sdu.edu.cn



Cheng-Xiang Wang (S'01-M'05-SM'08-F'17), received the BSc and MEng degrees in Communication and Information Systems from Shandong University, China, in 1997 and 2000, respectively, and the PhD degree in Wireless Communications from Aalborg University, Denmark, in 2004. He was a Research Assistant with the Hamburg University of Technology, Hamburg, Germany, from 2000 to 2001, a Visiting Researcher with Siemens AG Mobile Phones, Munich, Germany, in 2004, and a Research Fellow with the University of Agder, Grimstad, Norway, from 2001 to 2005. He has been with Heriot-Watt University, Edinburgh, U.K., since 2005, where

he was promoted to be a Professor in 2011. Since 2018, he joined Southeast University, China, as a Professor and Thousand Talent Plan Expert. He has authored 2 books, one book chapter, and over 330 papers in refereed journals and conference proceedings. His current research interests include wireless channel modeling and (B)5G wireless communication networks, including green communications, cognitive radio networks, high mobility communication networks, massive MIMO, millimetre wave communications, and visible light communications. Dr. Wang is a Fellow of the IET and HEA, and a member of the EPS-RC Peer Review College. He served or is currently serving as an Editor for nine international journals, including the IEEE TRANSACTIONS ON VEHICULAR TECHNOLOGY since 2011, the IEEE TRANSACTIONSON COMMUNICATIONS since 2015, and the IEEE TRANSACTIONS ON WIRELESS COMMUNICATIONS from 2007 to 2009. He was the leading Guest Editor of the IEEE JOURNAL ON SELECTED AREAS IN COMMUNICATIONS, Special Issue on Vehicular Communications and Networks. He is also a Guest Editor of the IEEE JOURNAL ON SELECTED AREAS IN COMMUNICATIONS, Special Issue on Spectrum and Energy Efficient Design of Wireless Communication Networks, and the IEEE TRANSACTIONS ON BIG DATA, Special Issue on Wireless Big Data. He served or is serving as a TPC Member, TPC Chair, and General Chair of over 80 international conferences. He received nine Best Paper Awards from the IEEE Globecom 2010, the IEEE ICCT 2011, ITST 2012, the IEEE VTC 2013, IWCMC 2015, IWCMC 2016, the IEEE/CIC ICC 2016, and the WPMC 2016. Email: chxwang@seu.edu.cn



Li Zhou, received Ph.D degree on 2004 from Zhejiang University, China. She has worked as project manager with Freescale Semiconductor R&D center till 2009. She participated in multiple National high-tech SoC and HDTV fundamental research projects, led multiple 65nm/90nm 10 million gate scale VLSI SoC chips, and joined many VLSI project and architecture researches. From 2009, Dr. Zhou worked as an assistant professor in Shandong University, China. Her current research interests include video processing system and hardware design, visible light communication, GPU architecture and VLSI design, embedded system and ASIC design, etc. Email: zhou_li@sdu.edu.cn